Neurobiology of Disease 218 (2026) 107205

Contents lists available at ScienceDirect

Neurobiology of Disease

journal homepage: www.elsevier.com/locate/ynbdi

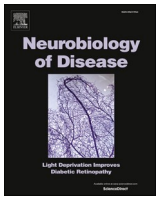

Modeling Mowat-Wilson syndrome with patient iPSCs reveals transcriptional and phenotypic defects in neural progenitors

Ilaria Musante [a], Giulia Gorrieri [a], Serena Tamburro [b], Giulia Ferrera [c,d], Simona Baldassari [a], Anna Fetta [e,f], Stefano Giuseppe Caraffi [g], Aglaia Vignoli [d,h], Giovanni Fiorito [i], Livia Garavelli [g], Maria Paola Canevini [c,d], Duccio Maria Cordelli [e,f], Federico Zara [a,b], Emilia Ricci [c,d,**], Paolo Scudieri [a,b,*]

[a] Medical Genetics Unit, IRCCS Istituto Giannina Gaslini, Genoa, Italy
[b] Department of Neurosciences, Rehabilitation, Ophthalmology, Genetics, Maternal and Child Health (DiNOGMI), University of Genoa, Genoa, Italy
[c] Child Neurology Unit-Epilepsy Center, San Paolo Hospital, Member of ERN-Epicare, Milan, Italy
[d] Department of Health Sciences, University of Milan, Milan, Italy
[e] U.O.C. Neuropsichiatria dell'età Pediatrica, IRCCS Istituto delle Scienze Neurologiche di Bologna, Bologna, Italy
[f] Dipartimento di Scienze Mediche e Chirurgiche (DIMEC), Alma Mater Studiorum, Università di Bologna, Bologna, Italy
[g] SOC Genetica Medica, Azienda USL-IRCCS di Reggio Emilia, Reggio Emilia, Italy
[h] Childhood Neurology and Psychiatry Unit, Azienda Socio Sanitaria Territoriale Grande Ospedale Metropolitano (ASST GOM) Niguarda, Milan, Italy
[i] Clinical Bioinformatics Unit, IRCCS Istituto Giannina Gaslini, Genoa, Italy

ARTICLE INFO

Keywords:
Disease models
Pluripotent stem cells
Neural induction
Cell motility

ABSTRACT

Zinc finger *E*-box-binding homeobox 2 (*ZEB2*) is a key transcription factor involved in multiple aspects of nervous system development, including neuronal specification, migration, and differentiation. Loss-of-function variants in *ZEB2* cause Mowat-Wilson syndrome (MWS), a severe neurodevelopmental disorder characterized by intellectual disability, epilepsy, and brain structural abnormalities. In this study, we generated and characterized induced pluripotent stem cell (iPSC) lines from MWS patients carrying pathogenic *ZEB2* variants. Patient-derived iPSCs retained full pluripotency and were capable of differentiating into all three germ layers, including neural lineages. Upon directed differentiation into neural progenitor cells (NPCs) and early neurons, we identified distinctive transcriptional alterations affecting neuroepithelial-to-radial glia transition and lineage specification. RNA-seq analysis revealed dysregulation of genes involved in cytoskeletal remodeling, extracellular matrix organization, and cell motility. Functional holographic live imaging confirmed a significant increase in motility behavior in MWS NPCs and early neurons, suggesting that altered cell dynamics may underlie aberrant neural circuit formation. Despite these changes, early neuronal markers such as MAP2 were expressed at comparable levels in MWS and control cells. Together, these findings uncover novel cellular and molecular phenotypes associated with *ZEB2* deficiency and provide insight into how disrupted progenitor behavior and transcriptional mis-regulation may contribute to the neurodevelopmental features of MWS.

1. Introduction

Zinc finger *E*-box-binding homeobox 2 (*ZEB2*), also known as SIP1 or ZFHX1B, encodes a transcription factor essential for multiple aspects of nervous system development, including progenitor cell fate specification, neuronal migration, and differentiation (Epifanova et al., 2019). While *ZEB2* primarily functions as a transcriptional repressor, it can also act as an activator depending on the cellular context and availability of specific cofactors (Epifanova et al., 2019). Its widespread expression is critical for the proper formation of both central and peripheral nervous system structures (Epifanova et al., 2019).

Germline haploinsufficiency of *ZEB2* causes Mowat-Wilson syndrome (MWS, MIM #235730), a rare congenital neurodevelopmental disorder characterized by facial dysmorphisms, agenesis/hypoplasia of

* Correspondence to: P. Scudieri, Medical Genetics Unit, IRCCS Istituto Giannina Gaslini, Genoa, Italy.
** Correspondence to: E. Ricci, Child Neurology Unit-Epilepsy Center, San Paolo Hospital, Member of ERN-Epicare, Milan, Italy.
E-mail addresses: emilia.ricci@asst-santipaolocarlo.it (E. Ricci), paolo.scudieri@unige.it (P. Scudieri).

https://doi.org/10.1016/j.nbd.2025.107205
Received 8 September 2025; Received in revised form 26 November 2025; Accepted 27 November 2025
Available online 29 November 2025

Table 1
Clinical details of MWS individuals selected for the generation of iPSC lines.

Patient ID	Sex (M/F)	Age at last follow up (years, months)	Growth parameters at birth// at last FU (percentile, SD)	Facial phenotype	Behavioral phenotype	Other clinical characteristics	Neurological examination at last follow up	Epilepsy (yes/no); age at onset (years, months)	Seizures types	EEG features at last follow up	MRI findings	ZEB2 pathogenic variant (cDNA, NM_014795.4; protein, NP_055610.1)
GGB11415F; previously published in (Cordelli et al., 2013) (pt 2); (Garavelli et al., 2017; Ivanovski et al., 2018) (pt 19); (Ricci et al., 2021) (pt 15), (Caraffi et al., 2024) (pt 18)	F	6	*W*: 30, −0.5 *H:* 58, +0.2 *HC:* 11, −1.2 // *W*: 57, +0.2 *H:* 73, +0.6 *HC*: 7, −1.5	Uplifted ear lobes, central depression of ear lobes, rounded skull, sparse hair, fine hair, large eyes, deep-set eyes, hypertelorism, telecanthus, broad nasal bridge, prominent columella, open mouth, M-shaped upper limb,	Frequent smiling, chewing/ mouthing objects or body parts, eating non-food items, grinding teeth, under-reaction to pain, rapid mood changes,	Slender, tapering fingers, long toes, genu valgus, broad, long halluces, overriding of toes, widely spaced teeth, delayed tooth eruption	Severe intellectual delay, motor stereotypies	Yes; 2,6	Focal, atypical absence	Slowing of background activity, fronto-central R spikes, occipital spikes	Partial agenesis of CC, dysmorphic hippocampal	c.2682del; p.(Leu894Phefs*36)
GGB28215F previously published in (Cordelli et al., 2013) (pt 19); (Ivanovski et al., 2018) (pt 62); (Ricci et al., 2021) (pt 17), (Caraffi et al., 2024) (pt 22)	F	15,2	*W*: 48, 00 *H:* na *HC*: na // *W:* 60, +0.3 *H*: 18, −0.9 *HC:* 1, −2.4	Microcephaly, large eyebrows, medially flaring eyebrows, sparse eyebrows in the middle, uplifted ear lobes, central depression of the ear lobes, rounded skull, fine hair, high forehead, large eyes, telecanthus, hypertelorism depressed nasal bridge, prominent columella, open mouth, M-shaped upper lip, elongation of the face depression of the nasal tip prognathism,	Frequent smiling, chewing/ mouthing object or body parts, grinding teeth, flickering/ tapening/ twirling objects, repetitive activities, standing too close to others, under-reaction to pain, excessive elation, rapid mood changes, laughing with no reason	Constipation, patent ductus arteriosus, ventricular septal defect, atrial septal defect, prominence of interphalangeal joints, astigmatism, widely spaced teeth, palmar and plantar creases, recurrent otitis media or other infections	Severe intellectual delay, motor stereotypies	Yes; 0,1	Focal, atypical absence, status epilepticus	Slowing of background activity, diffuse frontal dominant high voltage slow waves	Complete agenesis of CC, lateral ventricle enlargement	c.650_653dup; p.(Gly219Profs*21)
GGB11515M previously published in (Garavelli et al., 2017; Ivanovski et al., 2018) (pt 27); (Caraffi et al., 2024) (pt 19)	M	5, 11	*W*: 22, −0.8 *H:* 33, −0.4 *HC:* 15, −1 // *W*: 3, −2.0 *H*: 20, −0.9 *HC:* <1, −2.9	Microcephaly, sparse eyebrows in the middle, uplifted ear lobes, rounded skull, fine hair, high forehead, frontal bossing, large eyes, epicanthal folds, hypertelorism, telecanthus, broad nasal bridge, depressed nasal bridge, rounded nasal tip, prominent	Frequent smiling, chewing/ mouthing objects or body parts, flickering / tapening / twirling objects, grinding teeth, repetitive activity, under-reaction to pain, excessive elation,	Hirschsprung disease, Pyloric stenosis, patent ductus arteriosus, cryptorchidism, slender and tapering fingers, mild calcaneovalgus, pectus excavatum, superior pectus carinatum/ inferior pectus excavatum, adducted thumbs, hallux valgus, hypoplasia of toes middle and distal	Hypotonia, severe intellectual delay, motor stereotypies	Yes, 3	Focal, focal to bilateral tonic-clonic seizure	na	Partial agenesis of CC, ventricular temporal horn enlargement, reduction of thickness of WM	c.817del; p.(Leu273*)

(*continued on next page*)

Table 1 (*continued*)

Patient ID	Sex (M/F)	Age at last follow up (years, months)	Growth parameters at birth// at last FU (percentile, SD)	Facial phenotype	Behavioral phenotype	Other clinical characteristics	Neurological examination at last follow up	Epilepsy (yes/no); age at onset (years, months)	Seizures types	EEG features at last follow up	MRI findings	ZEB2 pathogenic variant (cDNA, NM_014795.4; protein, NP_055610.1)
				columella, open mouth, M-shaped upper lip, prominent chin	laughing with no reason	phalanges, overriding of the toes, strabismus, myopia, astigmatism, widely spaced teeth, recurrent otitis media or other infections						
GGB16117M previously published in (Ivanovski et al., 2018) (pt 89); (Caraffi et al., 2024) (pt 24)	M	4,10	*W:* 36, −0.4 *H:* 39, −0.3 *HC:* 20, −0.8 // *W:* 52, 0.0 *H:* 12, −1.2 *HC*: <1, −2.7	Microcephaly, large eyebrows, medially flaring eyebrows, sparse eyebrows in the middle, uplifted ear lobes, central depression of the ear lobes, frontal bossing, epicanthal folds, depressed nasal bridge, prominent columella, M-shaped upper lip, prominent chin	Frequent smiling, chewing / mouthing objects or body parts	Patent ductus arteriosus, pulmonary artery stenosis, ventricular septal defect, crossed pulmonary arteries, hypospadia, craniosynostosis (trigonocephaly), prominence of interphalangeal joints, pes planus, genu valgus, mild contractures of the hip/elbows/knees, broad halluces, hypermetropia, recurrent otitis media or other infections	severe intellectual delay	Yes; 3,6	Motor seizures not better defined (focal?)	na	Partial agenesis of CC	c.1578_1579delinsA; p.(Asp527Thrfs*17)

C = central; CC = corpus callosum; F = female; H = height; HC = head circumference; M = male; na = not available; O = occipital; R = right; W = weight; WM = white matter.

the corpus callosum, intellectual disability, and a high prevalence of epilepsy (75–85 % of individuals) (Mowat et al., 1998; Ivanovski et al., 2018; Cordelli et al., 2021). While early reports attributed epilepsy in MWS to structural brain anomalies (Engenheiro et al., 2008), more recent studies suggest also a genetically driven, cellular and circuit-level etiology. In a detailed electroclinical characterization, Ricci and colleagues described a stereotyped, age-dependent seizure progression (from febrile seizures in infancy to focal hypnic seizures and atypical absences, followed by remission in adolescence) with consistent responsiveness to valproate and no imaging findings typically associated with epileptogenic cortical malformation (Di Pisa et al., 2019; Ricci et al., 2021). These findings support the hypothesis that seizures in MWS also stem from more diffuse neurodevelopmental dysfunction. Interestingly, generalized epileptic discharges and absence seizures were frequently observed in patients with complete corpus callosum agenesis, suggesting that seizure propagation in MWS may involve cortical-subcortical circuits rather than interhemispheric pathways (Ricci et al., 2021). GABAergic inhibition has been proposed as a key regulator of such circuits, especially in seizure types like absence epilepsy (Galanopoulou, 2010; Miyamoto et al., 2019; Pfisterer et al., 2020). *ZEB2* has been shown to be crucial for the migration and fate specification of GABAergic interneurons derived from the medial ganglionic eminence (Epifanova et al., 2021; McKinsey et al., 2013; Takagi et al., 2015; van den Berghe et al., 2013). In mouse models, loss of *Zeb2* disrupts interneuron migration and alters their identity, leading to a shift from cortical to striatal fates and potentially contributing to excitation-inhibition imbalance (Epifanova et al., 2021; McKinsey et al., 2013; Takagi et al., 2015; Tomassy et al., 2013; van den Berghe et al., 2013). In addition to transcriptional dysregulation, abnormal neuronal morphology may also play a role in MWS epileptogenesis. *Zeb2* knockout mice display significantly shorter axons in cortical neurons compared to controls (Srivatsa et al., 2015), resembling defects reported in GABAergic neurons derived from SCN1A-mutated patients, which exhibit reduced dendritic arborization (Tiraboschi et al., 2020).

While these insights largely stem from animal models, patient-derived induced pluripotent stem cell (iPSCs) offer a unique and ethically feasible approach to study neural development and dysfunction in a human context. A pioneering iPSC-based study of *ZEB2* haploinsufficiency demonstrated impaired interneuron differentiation and altered gene expression (Schuster et al., 2022). However, due to the limited number of patient-derived lines available, further validation and expansion of these findings in additional models is needed to further elucidate the effects of *ZEB2* variants.

In this study, we sought to advance understanding of *ZEB2*-related neurodevelopmental dysfunction by generating and characterizing iPSC-derived neural progenitor cells (NPCs) from four unrelated individuals carrying pathogenic *ZEB2* variants. Transcriptomic profiling revealed dysregulation of genes involved in neuroepithelial-to-radial glia transition, lineage specification, cytoskeletal remodeling, and extracellular matrix interaction. In parallel, live-cell imaging demonstrated increased cell motility during early neuronal differentiation. Together, these findings provide novel molecular insights into *ZEB2*-associated neurodevelopmental dysfunction and reinforce the link between transcriptional dysregulation and epileptogenesis in MWS, thereby advancing our understanding of disease pathogenesis and identifying potential therapeutic targets.

2. Materials and methods

2.1. Cell reprogramming and culture conditions

Four MWS patients were selected for the generation of iPSC lines. Table 1 summarizes the clinical features of each individual with MWS. Peripheral blood mononuclear cells (PBMCs) were obtained from the Biobank of the Laboratory of Human Genetics – IRCCS Istituto Giannina Gaslini (a member of the Telethon Network of Genetic Biobanks, Project No. GTB18001) (Galliera Genetic Bank: A DNA and Cell Line Biobank from Patients Affected by Genetic Diseases, 2016). The following biobank ID numbers GGB11415F, GGB28215F, GGB11515M, and GGB16117M correspond to patients P1, P2, P3, and P4, respectively, in this study. As controls, we used two established iPSC lines derived from healthy individuals: C1 (female donor, age 1), originally described by Aprile et al., 2019 (Aprile et al., 2019), and C2 (male donor, age 1), a previously used and commercially available line (Musante et al., 2025).

Table 2
Primers used for Sanger sequencing and RT-PCR.

Target	Size (bp)	Forward and Reverse primer (5′-3′)
Primers for *ZEB2* variants validation		
c.2682del	234	AGATGAGCCTCTGAACTTGACT
		TGTGGTAGGAAGCTCATCTG
c.650_653dup	235	GCCCATTAGCTGCCATTGAT
		CGGTAGGCAAACGTGTAGC
c.817del	363	AGCATGCACTCAAACCTTTTG
		CAGGCACACAGAGTTGATGA
c.1578_1579delinsA	250	AGGATCCATGCTCTCAACCT
		ACTGGCATGAAAATGGAGTGG
Primers for RT-PCR of viral genes		
SeV	181	GGATCACTAGGTGATATCGAGC
		ACCAGACAAGAGTTTAAGAGATATGTATC
KOS	528	ATGCACCGCTACGACGTGAGCGC
		ACCTTGACAATCCTGATGTGG
Klf4	410	TTCCTGCATGCCAGAGGAGCCC
		AATGTATCGAAGGTGCTCA
c-Myc	532	TAACTGACTAGCAGGCTTGTCG
		TCCACATACAGTCCTGGATGATGATG
ATP5F1	575	TTAGCGCAGAGACCTTCACT
		CCAGTGCCTGTTGTGACTTC

For the reprogramming, PBMCs were thawed on day −4 and cultured at 37 °C with 5 % CO_2 in PBMC medium (StemPro™-34 SFM; 10,639,011, Thermo Fisher Scientific) supplemented with appropriate cytokines, following the recommendations of the Sendai viral transduction kit CytoTune-iPS 2.0 protocol (A1569601, Thermo Fisher Scientific). On the day of transduction, 3×10^5 PBMCs were counted and transduced with Sendai reprogramming vectors at MOI 5:5:3 (KOS, hc-Myc, hKlf4), following the manufacturer protocol (A1569601, Thermo Fisher Scientific). Briefly, cells and viruses were mixed in PBMC medium, centrifuged at 1000 ×*g* for 30 min at room temperature, and then transferred to one well of a 12-well plate. The plate was incubated overnight at 37 °C and 5 % CO_2. The following day, the medium containing viruses was removed by centrifuging the cell suspension at 200 ×*g* for 10 min. Cells were then resuspended in 0.5 ml of complete PBMC medium per well of a 24-well plate. At day 3 after transduction, 1×10^4 to 1×10^5 live cells were plated onto Geltrex™-coated (A1413302, Thermo Fisher Scientific) 6-well plates in 2 ml of PBMC medium without the cytokines. Every other day, half of the spent medium was gently removed and replaced with 1 ml of fresh StemPro™-34 medium without cytokines until day 7. At day 8, PBMC medium was replaced with Essential 8™ Medium (A1517001, Thermo Fisher Scientific) until iPSC colonies appeared. From day 15 post-transduction, colonies were ready for picking and were transferred into Geltrex-coated 12-well plates in Essential 8™ Medium, which was subsequently replaced with Essential 8™ Flex Medium (A2858501, Thermo Fisher Scientific). Colonies were cultured until passage 10 on Geltrex-coated 6-well plates in Essential 8™ Flex Medium at 37 °C with 5 % CO_2. Cells were passaged every 2–3 days at a ratio of 1:5 to 1:10 using Versene solution (15,040,066, Thermo Fisher Scientific). During passaging and thawing steps, the medium was supplemented overnight with RevitaCell™ (A2644501, Thermo Fisher Scientific) overnight. Cell freezing was performed using Bambanker (BB01, NIPPON Genetics EUROPE).

Table 3
Antibodies used for immunofluorescence.

Target	Catalog number	Dilution
OCT4	703,927, Thermo Fisher Scientific	1:500
SSEA-4	MA1–021, Thermo Fisher Scientific	1:500
TRA-1-60	MA1–023, ThermoFisher Scientific	1:250
SOX2	14–9811-82, Thermo Fisher Scientific	1:250
PAX6	MA1–109, Thermo Fisher Scientific	1:200
β3-tubulin	302,304, Synaptic Systems	1:200
TBXT	14–9770-82, Thermo Fisher Scientific	1:100
TBX6	BS-12281R, Thermo Fisher Scientific	1:100
SOX17	MA5–24885, Thermo Fisher Scientific	1:50
FOXA2	701,698, Thermo Fisher Scientific	1:100
SOX1	MA5–32447, Thermo Fisher Scientific	1:200
MAP2	188,004, Synaptic Systems	1:500

2.2. Genetic analysis of iPSC lines

The presence of the expected *ZEB2* variants in the newly generated iPSC lines was verified by Sanger sequencing, while array-CGH with the SurePrint G3 Human CGH Microarray Kit 180 K (G4449 A, Agilent) detected no chromosomal rearrangements. The complete array-CGH datasets will be made available upon request.

Genomic DNA was extracted from PBMCs and iPSCs using the QIAmp DNA micro kit (56,304, Qiagen). DNA concentration was measured with NanoDrop 1000 spectrophotometer (Thermo Fisher Scientific). 100 ng of total DNA was used to perform PCR using the AmpliTaq Gold™ 360 Master Mix. The sequences of forward and reverse primers used are listed in Table 2. The PCR products, purified using ExoSAP-IT (78,201, Applied Biosystems), were subjected to sequencing PCR with BigDye Terminator v1.1 Cycle Sequencing kit (4,336,774, Applied Biosystems), according to manufacturer's instructions. Then, capillary electrophoresis by ABI PRISM 310 Genetic Analyzer (Thermo Scientific) was performed to obtain sequences electropherograms.

2.3. Reverse transcription PCR (RT-PCR)

RT-PCR on iPSCs at passage 10 was performed to verify the loss of exogenous factor genes. For this purpose, RNA extraction was performed using RNeasy Mini Kit (74,104, Qiagen), according to the manufacturer's protocol. The RNA concentration was measured with NanoDrop 1000 spectrophotometer (Thermo Fisher Scientific). 250 ng of total RNA was used for cDNA synthesis with iScript™ cDNA Synthesis Kit (1,708,891, Biorad). cDNA was used to perform PCR using the AmpliTaq Gold™ 360 Master Mix (4,398,881, Thermo Fisher Scientific). PCR products were separated by electrophoresis on a 2 % agarose gel containing EuroSafe Nucleic Acid Stain (EMR440001, Euroclone) and visualized under UV illumination using a Mini HD9 system (Uvitec Cambridge). The sequences of forward and reverse primers used are listed in Table 2.

2.4. Trilineage differentiation

To assess pluripotency, iPSC lines were subjected to directed differentiation into mesoderm, endoderm, and ectoderm lineages using the STEMdiff™ Trilineage Differentiation Kit (05230, STEMCELL Technologies), according to the manufacturer's instructions. Briefly, iPSCs were plated onto Geltrex™-coated 8-chamber slides (80,841, IBIDI) and cultured in lineage-specific induction media. Endodermal and mesodermal differentiation was carried out over 5 consecutive days, while ectodermal differentiation was performed over 7 days, with daily medium changes for all conditions. At the end of the differentiation period, cells were fixed with 10 % neutral buffered formalin (05-01005Q, Bio-Optica) and subjected to immunofluorescence analysis using antibodies targeting lineage-specific markers for each germ layer, as described in the following section and listed in Table 3.

2.5. Generation of iPSC-derived neural progenitor cells (NPC)

iPSC-derived NPCs were generated via dual inhibition of SMAD signaling using the STEMdiff Neural System (STEMCELL Technologies), following the manufacturer's instructions and as previously described in (Musante et al., 2025). Briefly, iPSC colonies were detached by incubating with StemPro™ Accutase™ Cell Dissociation Reagent (A1110501, Thermo Fisher Scientific) for 5 min. The cells were then collected by gentle pipetting in DMEM/F12 medium (11,330,057, Thermo Fisher Scientific) to obtain a single-cell suspension. Following centrifugation at 300 $\times g$ for 5 min, the cells were resuspended in STEMdiff™ Neural Induction Medium + SMADi (08581, STEMCELL Technologies) supplemented with RevitaCell™ (A2644501, Thermo Fisher Scientific). A total of 3×10^6 cells were seeded into each well of an AggreWell™ 800 plate (34,811, STEMCELL Technologies) in a final volume of 2 ml. The plate was centrifuged at 100 $\times g$ for 3 min to facilitate cell capture in the microwells, and three-quarters of the medium was replaced daily for 5 days. During this period, iPSCs aggregated at the bottom of the wells to form embryoid bodies (EBs). These EBs were then collected and plated onto 6-well plates coated with Geltrex™ (A1413302, Thermo Fisher Scientific) and cultured for an additional 7 days to allow the formation of neural rosettes. Subsequently, neural rosettes were detached using STEMdiff™ Neural Rosette Selection Reagent (05832, STEMCELL Technologies) and transferred to a Geltrex-coated well of a 6-well plate. NPCs emerging from the neural rosettes were cultured for 5–7 days. To obtain a single-cell suspension, NPCs were dissociated using Accutase and transferred to a 6-well plate in STEMdiff™ Neural Progenitor Medium (05833, STEMCELL Technologies) at a density of 1×10^6 cells per well, defined as NPC passage 1. NPCs were expanded and maintained by feeding every other day with Neural Progenitor Medium.

2.6. Generation of NPC-derived early neurons

NPCs were plated in STEMdiff Neural Progenitor medium on Geltrex-coated 24-well plates (82,426, IBIDI) at a density of 4×10^4 cells/well. After 24 h, the medium was replaced with Neurobasal Medium (21,103,049, Thermo Fisher Scientific) supplemented with GlutaMax Supplement (1:100), B-27 supplement (1:50), BDNF (10 ng/ml), GDNF (10 ng/ml), retinoic acid (1 μM), ascorbic acid (200 μM) and CulturOne supplement (1:100). Half of the medium was replaced twice a week during continuous culturing. From day 5 (d5) onward, Neurobasal Medium and B-27 supplement were substituted by Neurobasal Plus Medium (A3582901, Thermo Fisher Scientific) and B-27 Plus supplement (A3582801, Thermo Fisher Scientific), respectively. Throughout the differentiation period, NPC-derived neurons were monitored using label-free holographic imaging and were fixed at day 10 (d10) with 10 % neutral buffered formalin for subsequent immunofluorescence analysis.

2.7. Immunofluorescence analysis

Control and MWS cells were subjected to immunofluorescence detection and quantification of specific markers to verify proper progression through key developmental stages: undifferentiated state (OCT4, SSEA-4, TRA-1-60, and SOX2) and pluripotency/trilineage differentiation (PAX6 and β3-tubulin for ectoderm, TBXT and TBX6 for mesoderm, and SOX17 and FOXA2 for endoderm) of iPSC lines, neural identity of iPSC-derived neural progenitor cells (SOX1 and PAX6), and early neuronal maturation (MAP2).

Cells were washed in PBS and fixed with 10 % neutral buffered formalin (05-01005Q, Bio-Optica) for 5 min at room temperature. After three washings in PBS, cells were permeabilized with Triton X-100 0.3 % in PBS for 5 min, blocked with 1 % BSA in PBS for 2 h, and then incubated overnight at 4 °C with a solution of primary antibodies diluted in PBS containing 1 % BSA. Antibody details, including catalog numbers and dilutions, are listed in Table 3. Following incubation with primary

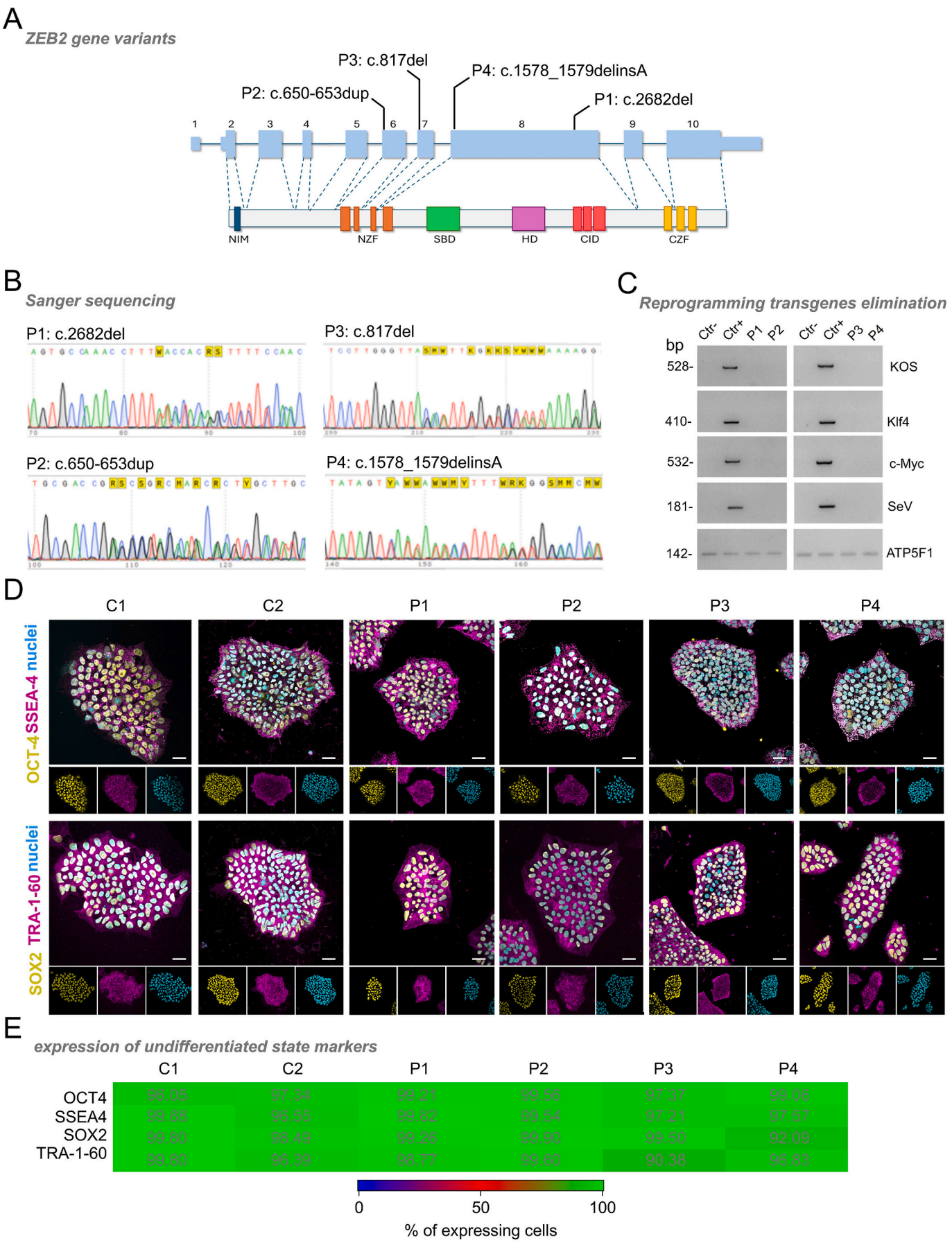

(caption on next page)

Fig. 1. Generation of MWS iPSCs carrying ZEB2 variants. (A) Schematic representation of the ZEB2 gene and its encoded protein. Positions of the mutations identified in patients P1–P4 are indicated. (B) Sanger sequencing traces confirming the presence of ZEB2 variants in the selected iPSC clones. (C) RT-PCR analysis showing the loss of exogenous viral gene expression. PCR products were separated by agarose gel electrophoresis. The first two lanes represent cDNA from PBMCs before (Ctr-) and after (Ctr+) delivery of reprogramming viruses. Lanes P1-P4 correspond to patient-derived iPSC clones at passage 10, which no longer express the reprogramming transgenes (KOS, Klf4, c-MYC, SeV). ATP5F1 was used as a housekeeping control. (D, E) Representative confocal images (D) and heatmap (E) showing the expression of undifferentiated state markers in control (C1, C2) and patient-derived iPSC lines. Immunofluorescence analysis was performed for OCT4, SSEA4, SOX2, and TRA-1–60. Scale bar: 25 μm. A total of $n = 2000$ cells were analyzed at the passage preceding cell banking and neural induction, with >90 % of cells expressing each marker (values indicated in heatmap).

antibodies, cells were rinsed three times in PBS and incubated with a solution of secondary Alexa Fluor–conjugated antibodies (Thermo Fisher Scientific) diluted 1:200 in PBS containing 1 % BSA for 1 h in the dark. After further three washes in PBS, the slides were mounted with Fluoroshield with DAPI to stain cell nuclei.

Image acquisition was performed using a laser scanning confocal microscope TCS SP8 (Leica Microsystems) and an Eclipse TiE automated microscope (Nikon) to acquire high-resolution representative images and for quantitative analysis, respectively. Image analysis was performed using the General Analysis package in NIS Elements AR software as detailed in Musante et al., 2025 (Musante et al., 2025). Nuclear morphology was assessed on DAPI-stained images by measuring nuclear area and circularity using the same software package.

2.8. QuantSeq 3′ mRNA sequencing library preparation

Transcriptomic analysis was performed on 4 separate preparations of NPCs derived from MWS-iPSC lines (P1-P4) and two control iPSC lines (C1, C2). Total RNA was extracted using the RNeasy Mini Kit (74,104, Qiagen), following the manufacturer's protocol. RNA concentration was quantified using the Qubit 4.0 Fluorometer (Thermo Fisher Scientific) and adjusted to 10 ng/μL.

Libraries were prepared from 125 ng of total RNA using the NEGEDIA Digital mRNA-seq research grade sequencing service v2.0 (Next Generation Diagnostic srl) which included library preparation, quality assessment, and sequencing. Sequencing was performed on a NovaSeq 6000 system (Illumina Inc.) using a single-end, 100-cycle strategy.

2.9. QuantSeq 3′ mRNA sequencing data processing and analysis

Raw sequencing data were analyzed using the proprietary NEGEDIA Digital mRNA-seq pipeline (v2.0) provided by Next Generation Diagnostic srl. The pipeline includes quality filtering and trimming, alignment to the reference genome, and gene-level read counting. Normalization and differential expression analysis were performed using the NEGEDIA degsanalysis pipeline (v1.2.0). Specifically, sequence reads were trimmed using BBDuk software to remove adapter sequences, poly-A tails, and low-quality end bases. Alignment was performed with STAR 2.6.0a on hg38 reference genome assembly. Gene expression levels were determined using HTseq-counts 0.9.1. Differentially expressed genes (DEGs) were identified using the following thresholds: $\log_2$(Fold Change) ≥ 1.5 or ≤ -1.5 and adjusted p-value (pAdj) ≤ 0.05. A total of 43 significantly downregulated and 116 significantly upregulated genes in MWS cells compared to controls are listed in Supplementary File.

Gene Ontology (GO) enrichment analysis was performed on these DEGs using the ShinyGO v.0.82 online tool (Ge et al., 2020) restricting the output to Biological Process, Cellular Component, Molecular Function, and KEGG categories. A false discovery rate (FDR) cutoff of <0.05 was applied for term selection. All transcripts detected in the experiment were used as the background set.

2.10. Accession codes

The RNA-seq data discussed in this publication have been deposited in NCBI's Gene Expression Omnibus and are accessible through GEO Series accession number GSE311389 (https://www.ncbi.nlm.nih.gov/geo/query/acc.cgi?acc=GSE311389).

2.11. Holographic imaging and analysis

Label-free live imaging of NPCs and neurons seeded on Geltrex-coated 24-well plates (82,426, IBIDI) was performed using the Holomonitor M4 imaging system, equipped with a motorized xyz-stage and 20× objective (Phase Holographic Imaging PHI AB). Live-cell holographic imaging was conducted according to the manufacturer's instructions. For NPCs, images were acquired every 10 min over a total duration of 16 h. During neuronal differentiation, images were captured every 30 min for a total of 65 h between medium changes.

Image processing and analysis were performed with APP Suite Cell Imaging Software (Phase Holographic Imaging PHI AB), employing the Kinetic Cell Motility, Kinetic Cell Proliferation, and Cell Quality Control assays. Cell segmentation and identification were automatically performed using an adaptive Gaussian threshold method with a threshold value set at 135 and a minimum cell size of 16, consistently applied across all wells and positions. The following dynamic and morphological features were quantified: cell count, confluence, mean cell volume, mean cell area, mean cell diameter, mean cell speed, accumulated cell distance.

2.12. Data presentation and statistical analysis

All graphs and figures were generated using Igor Pro 9 (WaveMetrics). Data are presented as representative images and quantitative graphs displaying individual data points along with the mean ± S.D., obtained from independent biological replicates. The exact number of biological replicates for each experiment is specified in the corresponding figure legends. Statistical analyses were performed by grouping data according to condition (C1 and C2 as controls; P1-P4 as patient-derived lines). The association of marker expression, genes, and other cell measures, such as mean cell speed, volume, area, etc., with case-control status was tested using linear mixed-effects regression models. The cell status (case-control) was included as a fixed effect, while cell ID was treated as a random effect to take into account the repeated measurements associated with the same cell line. Analyses were conducted using the *lmer* function within the *lme4* package (version 1.1–37) in R.

3. Results

3.1. Generation and validation of iPSC lines carrying ZEB2 variants

We successfully generated iPSCs from four MWS patients carrying distinct pathogenic variants in the *ZEB2* gene, each associated with well-documented clinical phenotypes (Table 1). The following variants (all referred to transcript NM_014795.4) were modelled: c.2682del (P1), c.650_653dup (P2), c.817del (P3), and c.1578_1579delinsA (P4). Variants in patients P1 and P4 are in exon 8, while those in P2 and P3 reside in exons 6 and 7, respectively (Fig. 1A). All variants introduce frameshifts predicted to trigger nonsense-mediated mRNA decay, consistent with *ZEB2* haploinsufficiency. PBMCs were reprogrammed using a standard Sendai virus-based protocol. Sanger sequencing confirmed the presence of the *ZEB2* variants in the iPSC clones, and RT-PCR analysis verified the loss of exogenous reprogramming factor expression (Fig. 1B,